narra j

Original Article

Optimizing antimicrobial synergy: Green synthesis of silver nanoparticles from *Calotropis gigantea* leaves enhanced by patchouli oil

Pati Kemala[1], Khairan Khairan[2,3,4], Muliadi Ramli[2], Zuchra Helwani[5], Asep Rusyana[6], Vanizra F. Lubis[3], Khairunnas Ahmad[2], Ghazi M. Idroes[1,7], Teuku R. Noviandy[8] and Rinaldi Idroes[2,3,4*]

[1]Graduate School of Mathematics and Applied Sciences, Universitas Syiah Kuala, Banda Aceh, Indonesia; [2]Department of Chemistry, Faculty of Mathematics and Natural Sciences, Universitas Syiah Kuala, Banda Aceh, Indonesia; [3]Department of Pharmacy, Faculty of Mathematics and Natural Sciences, Universitas Syiah Kuala, Banda Aceh, Indonesia; [4]Pusat Riset Obat Herbal, Universitas Syiah Kuala, Banda Aceh, Indonesia; [5]Department of Chemical Engineering, Universitas Riau, Pekanbaru, Indonesia; [6]Department of Statistics, Faculty of Mathematics and Natural Sciences, Universitas Syiah Kuala, Banda Aceh, Indonesia; [7]Department of Occupational Health and Safety, Faculty of Health Science, Universitas Abulyatama, Aceh Besar, Indonesia; [8]Department of Informatics, Faculty of Mathematics and Natural Sciences, Universitas Syiah Kuala, Banda Aceh, Indonesia

*Corresponding author: rinaldi.idroes@usk.ac.id

Abstract

Silver nanoparticles (AgNPs) synthesized from plant extracts have gained attention for their potential applications in biomedicine. *Calotropis gigantea* has been utilized to synthesize AgNPs, called AgNPs-LCg, and exhibit antibacterial activities against both Gram-positive and Gram-negative bacteria as well as antifungal. However, further enhancement of their antimicrobial properties is needed. The aim of this study was to synthesize AgNPs-LCg and to enhance their antimicrobial and antifungal activities through a hybrid green synthesis reaction using patchouli oil (PO), as well as to characterize the synthesized AgNPs-LCg. Optimization was conducted using the response surface method (RSM) with a central composite design (CCD). AgNPs-LCg were synthesized under optimal conditions and hybridized with different forms of PO—crude, distillation wastewater (hydrolate), and heavy and light fractions—resulting in PO-AgNPs-LCg, PH-AgNPs-LCg, LP-AgNPs-LCg, and HP-AgNPs-LCg, respectively. The samples were then tested for their antibacterial (both Gram-positive and Gram-negative bacteria) and antifungal activities. Our data indicated that all samples, including those with distillation wastewater, had enhanced antimicrobial activity. HP-AgNPs-LCg, however, had the highest efficacy; therefore, only HP-AgNPs-LCg proceeded to the characterization stage for comparison with AgNPs-LCg. UV-Vis spectrophotometry indicated surface plasmon resonance (SPR) peaks at 400 nm for AgNPs-LCg and 360 nm for HP-AgNPs-LCg. The Fourier-transform infrared spectroscopy (FTIR) analysis confirmed the presence of O-H, N-H, and C-H groups in *C. gigantea* extract and AgNP samples. The smallest AgNPs-LCg were 56 nm, indicating successful RSM optimization. Scanning electron microscopy (SEM) analysis revealed spherical AgNPs-LCg and primarily cubic HP-AgNPs-LCg, with energy-dispersive X-ray spectroscopy (EDX) confirming silver's predominance. This study demonstrated that PO in any form significantly enhances the antimicrobial properties of AgNPs-LCg. The findings pave the way for the exploration of enhanced and environmentally sustainable antimicrobial agents, capitalizing on the natural resources found in Aceh Province, Indonesia.

Keywords: Antibacterial, antifungal, metal nanoparticle, *Pogostemon cablin*, essential oil

https://narraj.org/

Received: April 18, 2024 - Accepted: June 19, 2024 - Published online: June 20, 2024

Introduction

The rapid emergence of bacterial resistance, spurred by genetic adaptations, has outpaced the development of new antibiotic classes, with no major breakthroughs in nearly three decades [1]. In response, the focus has shifted towards natural resources, valued for their safety, eco-friendliness, and cost-effectiveness [2,3]. This pivot has sparked extensive research into plant secondary metabolites as potential antibacterial [4-8], antifungal [9,10], antiviral [11-13], and anticataract [14], driven by the hope of discovering effective new antibiotics.

Nanoparticles composed of both metals and non-metals are an area of nanotechnology research that has seen significant development within the medical field [15-18]. Metal nanoparticles biologically synthesized using bioagents such as plants, fungi, and bacteria typically exhibit reduced toxicity to eukaryotic cells. This characteristic presents potential applications in the field of biomedicine. The antimicrobial properties of metallic silver have been recognized for centuries, and it has been used in various medical devices [19]. Currently, silver nanoparticles (AgNPs) are considered a primary alternative antimicrobial agent for effective microbial control [20]. Green synthesis of AgNPs offers opportunities for novel biomedical innovations, including in the area of nanomedicine [21]. AgNPs are known to induce structural and physiological damage to microbial cell membranes, leading to altered membrane permeability and inhibition of respiratory proteins. These changes disrupt cell homeostasis, ultimately resulting in the destruction of microbial cells [22]. Various plants have been reported for the synthesis of AgNPs, including *Picea abies* [23], *Zingiber officinale* [24], *Nigella sativa* [24], *Plumbago auriculata* [25], *Hypericum perforatum* [26], *Syzigyum cymosum* [27], *Lippia abyssinica* [28], *Zizyphus mauritiana* [29] and *Calotropis gigantea* [30-33]. A recent study has shown that coating AgNPs synthesized with water hyacinth (*Lablab purpureus*) seed extract using patchouli oil (PO) enhances its antibacterial activity against *E. coli* [34]. PO is known to form a protective layer on AgNPs, preventing agglomeration and oxidation, thereby improving their antibacterial efficacy [34]. Notably, PO, extracted from *Pogostemon cablin* Benth (*P. cablin)* leaves, is a significant product of Aceh Province, the world's largest PO supplier [35]. In our previous study, AgNPs were successfully synthesized using *C. gigantea*, an endemic plant from a geothermal area [36]. Notably, *C. gigantea* from this region is enriched with secondary metabolites like alkaloids, steroids, tannins, phenolics, and saponins [37,38]. Our previous study demonstrated the antimicrobial activities of AgNPs synthesized using extracts from *C. gigantea* leaves (AgNPs-LCg) and flowers (AgNPs-FCg) against *Staphylococcus aureus, Escherichia coli,* and *Candida albicans)* [36]. AgNPs-LCg had inhibition zones of 10.60 mm, 8.40 mm, and 8.90 mm against Gram-positive bacteria (*S. aureus*), Gram-negative bacteria (*E. coli*), and *C. albicans*, respectively. Meanwhile, AgNPs-FCg exhibited stronger inhibition against these pathogens [36].

The aim of this study was to optimize the synthesis of AgNPs-LCg, aiming to enhance their antimicrobial properties and assess their efficacy against various microorganisms, with focusing on incorporating PO for further enhancement. To the best of our knowledge, a study on enhancing the antimicrobial activity of AgNPs synthesized using *C. gigantea* with PO has not yet been conducted. This study introduces a novel and sustainable approach to AgNP synthesis by leveraging the unique properties of *C. gigantea* leaves, a plant indigenous to the geothermal area of Ie Seu-um, Aceh Besar District, Aceh Province, Indonesia. The utilization of green synthesis methods aligns with the growing demand for eco-friendly nanomaterial production. The optimization of antimicrobial activity through the hybridization of AgNPs with different forms of PO, including crude oil, distillation wastewater (hydrolate), and heavy and light fractions. This research contributes to the advancement of sustainable nanotechnology applications with potential implications for biomedical and environmental sectors.

Methods

Study design and setting

In this study, *C. gigantea* was extracted prior to being used as a bioreductant in the green synthesis of AgNPs. The response surface method (RSM) was employed for reaction optimization. The effects of the independent variables ($AgNO_3$ concentration and pH) on the surface plasmon

resonance (SPR) peak were examined using a UV-Vis spectrophotometer. The optimum reaction conditions identified were then used as a reference for the green synthesis hybrid process of producing AgNPs-LCg coated with various forms of PO (crude oil, distillation wastewater (hydrolate), and heavy and light fractions). These samples were then tested for their antimicrobial activity against Gram-positive bacteria (*S. aureus*), Gram-negative bacteria (*E. coli*), and fungi (*C. albicans*). Characterization of AgNPs was conducted using UV-Vis spectrophotometry, Fourier-transform infrared spectroscopy (FTIR), particle size analyzer (PSA) and scanning electron microscopy energy-dispersive X-ray spectroscopy (SEM-EDS) instruments.

Sample collection

C. gigantea samples were collected from the Ie Seu-um geothermal area in Aceh Besar District, Aceh Province, Indonesia. The precise coordinates of the sampling location were N05°32'50.97", E095°32'55.10', situated at an elevation of 97 meters above sea level. The collected samples were washed to remove impurities and then hand-cut. The leaf samples were dried at room temperature for three days before proceeding to the extraction process. During extraction, 10 g dried leaves were boiled in 100 mL of distilled water for 20 min and subsequently filtered using filter paper. The filtrate was preserved at 4°C for later use. This extraction method and solvent usage followed protocols established in previous studies [30,31,36,39].

PO was sourced from local farmers in Kota Sabang, Aceh Province, Indonesia. The crude PO underwent purification using a rotary evaporator to separate it into light and heavy fractions [40]. Initially, the fractionation process commenced within a temperature range of 60°C to 65°C at a pressure of 2 Mbar. To mitigate the risk of bumping, the temperature was increased every 5 to 10 min until it reached 125°C. This stage culminated in the extraction of the light fraction of PO. Subsequently, the process was extended to obtain the high fraction, with fractionation continuing until the temperature varied between 115°C and 160°C [41]. These four types of PO—crude, hydrolate, light fraction, and heavy fraction—were utilized as coatings in the hybrid green synthesis process of this study. The different types of POs used are depicted in an illustration provided in **Figure 1**.

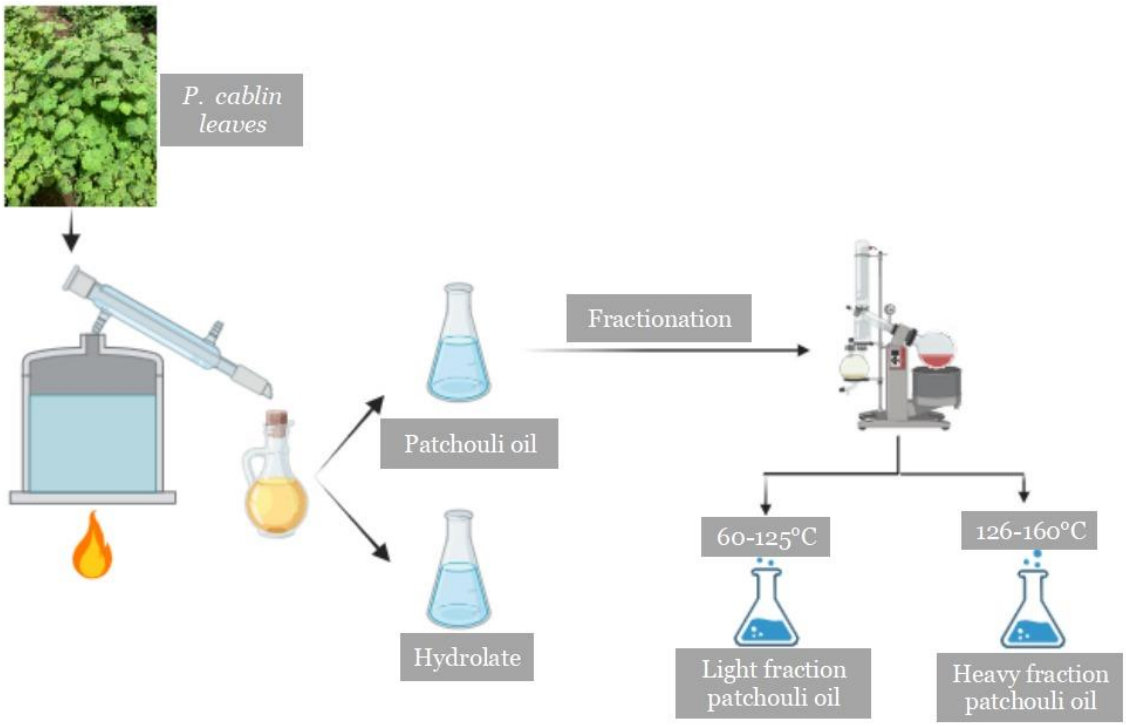

Figure 1. Types of patchouli oil (PO) samples used for the green synthesis hybrid of AgNPs-LCg and how they were produced.

Green synthesis AgNPs-LCg

AgNPs were synthesized by slightly modifying the method described by Sorubavalli *et al.* [32], wherein 10 mL of leaf extract was combined with 90 mL of $AgNO_3$ solution. The reaction process

was conducted in darkness and continuously stirred at 60 rpm using a magnetic stirrer for 48 h. After mixing the extract and $AgNO_3$ solution, the color of the reaction mixture gradually changed to a brown colloidal suspension, indicating the reduction process of Ag^+ ions to Ag metal NPs with the phytochemical contribution of plant extract [41]. Variations in the concentration of $AgNO_3$ and adjustments in pH were made in accordance with the RSM design (**Table 1**). The pH was adjusted using 0.1 N HCl and NaOH solutions. To prevent the photoactivation of silver nitrate, incubation was conducted in the absence of light, as recommended previously by Sharma *et al.* [42]. After a 48-hour incubation period, the reaction was terminated. The absorbance of the solution was measured using UV-Vis spectrophotometry across a wavelength range of 300–600 nm. The SPR value obtained was then utilized as the response data in the RSM analysis. Subsequently, the solution underwent centrifugation (Nuve, NF 800R model, Ankara, Turkey) for 30 min to yield AgNP pellets.

Design of experiment (DoE) based optimization

Optimal reaction conditions were established using the concentration of $AgNO_3$ and pH as independent variables. These parameters were input into Minitab 18.0 to execute RSM utilizing a central composite design (CCD) approach. The patterns of randomization implemented are detailed in **Table 1**.

Table 1. Central composite design (CCD)

Runs	Variable code ($AgNO_3$)	Variable code pH	$AgNO_3$	pH	Experimental surface plasmon resonance (SPR)
1	1.414	0	9.242	8	480
2	0	1.414	5	13.6	480
3	1	-1	8	4	490
4	0	0	5	8	520
5	-1	-1	2	4	460
6	0	0	5	8	520
7	0	0	5	8	520
8	-1	1	2	12	510
9	0	0	5	8	520
10	0	0	5	8	520
11	0	-1.414	5	2.32	460
12	1	1	8	12	470
13	-1.414	0	0.758	8	500

Green synthesis hybrid AgNPs-LCg using patchouli

The green synthesis of hybrid AgNPs-LCg using PO began with the preparation of AgNPs-LCg under optimal reaction conditions recommended by the RSM. However, after 24 h of incubation, 4 mL of crude PO was added, and the reaction was then allowed to continue for a total incubation period of 48 h. The reaction was repeated by replacing crude PO with three other types of PO, resulting in a total of four samples. AgNPs-LCg hybridized with crude PO and its hydrolate were designated as PO-AgNPs-LCg and PH-AgNPs-LCg, respectively. It should be noted that hydrolate was the wastewater by-product generated during the distillation process of PO, as depicted in **Figure 1**. Furthermore, AgNPs-LCg hybridized with the light and heavy fractions of PO were labeled as LP-AgNPs-LCg and HP-AgNPs-LCg, respectively.

Antimicrobial activity assay

Antimicrobial activity tests were conducted against *S. aureus* (a Gram-positive bacterium), *E. coli* (a Gram-negative bacterium), and the fungus *C. albicans* using the Kirby-Bauer disc diffusion method. The bacterial strains used in this study were *S. aureus* (ATCC 25923) and *E. coli* (ATCC 25922), while the fungal strain was *C. albicans* (ATCC 10231). The test samples included *C. gigantea* leaf extract, PO, AgNPs-LCg, a positive control, and four samples of green synthesized AgNPs-LCg hybridized with various patchouli samples (PO-AgNPs-LCg, PH-AgNPs-LCg, LP-AgNPs-LCg, and HP-AgNPs-LCg).

Both *S. aureus* and *E. coli* were cultured in Mueller-Hinton agar (MHA) media at 37°C for 24 h. Subsequently, colonies from the liquid media were spread on petri dishes containing MHA agar using a spreader. Sterile paper discs (6 mm in diameter) were then placed on these Petri dishes for inoculation. AgNps-LCg, *C. gigantea* leaf extract, PO-AgNPs-LCg, PH-AgNPs-LCg, LP-

AgNPs-LCg, HP-AgNPs-LCg, crude PO and controls were applied to each paper disc. Vancomycin was used as the positive control for Gram-positive, while gentamicin was used for Gram-negative bacteria. The diameter of the inhibition zones was measured after 24 h of incubation at 37°C. Similarly, antifungal activity against *C. albicans* was assessed using the same methodology but with Sabouraud dextrose agar (SDA) media, and ketoconazole was used as positive control for antifungal test. The experiment was conducted with three replicates for each test.

Characterization

UV-Vis characterization is a commonly employed method to assess the formation of AgNPs [2]. These nanoparticles are known to absorb and scatter specific wavelengths of visible light, a phenomenon commonly referred to as SPR [22,43]. The presence of an SPR absorbance peak is indicative of nanoparticles being uniformly dispersed in the solution [42]. AgNPs-LCg and AgNPs obtained from the hybrid green synthesis had the highest antimicrobial activity and therefore were further characterized with several instruments including UV-Vis spectrophotometer (Shimadzu, UV 2500, Shimadzu Suzhou Instruments Mfg. Co., Ltd., Jiangsu, China) to measure the SPR peaks of the samples. To determine the functional groups of *C. gigantea* involved in the Ag reduction process, characterization was performed using Fourier transform infrared (FTIR) spectroscopy (Search 630 FTIR Spectrometer, Agilent Technologies, Santa Clara, CA, USA). The size measurement of the samples was conducted using particle size analyzer (Shimadzu SALD-2300, Japan). The morphology of AgNPs was characterized using scanning electron microscopy energy-dispersive X-ray spectroscopy (SEM-EDS, Carl Zeiss-Bruker EVO MA 10, Carl Zeiss Microscopy, White Plains, NY, USA).

Statistical Analysis

The experiments were conducted in triplicate, and the results are expressed as the mean value with the standard deviation. Statistical analysis was performed using ANOVA at a significance level of 0.05. Additionally, Duncan's test was employed to identify significant differences between pairs of data.

Results

Sample preparation

The resultant *C. gigantea* leaf extract was greenish-yellow in color (**Figure 2A**) and resultant color of AgNPs-LCg was predominantly dark brown. A comparison of the solution's color before and after incubation is illustrated in **Figure 2B** and **Figure 2C**. The hybrid green synthesis of AgNPs-LCg was carried out by adding the different forms of PO—crude, distillation wastewater (hydrolate), and heavy and light fractions midway through the reaction. The resulting solution after the addition of PO to the four types of hybrid AgNPs appeared brown (**Figure 2D**) but was not homogeneous, due to the presence of undissolved oil.

Design of experiment (DoE) based optimization

The research uses a response surface design with CCD to identify the maximum SPR value. Besides that, the research also uses ANOVA of complete random design with one factor. The experimental data, analyzed through ANOVA, are concisely presented in **Table 2**. To evaluate the validity, significance, and acceptability of the mathematical model generated via regression techniques, we utilized the probability value (*p*-value) and the Fisher test value (*F*-value). The high *F*-value of the resulting regression model indicates its reliability.

The model of the design is: $y_{ij} = \mu + \tau_i + \varepsilon_{ij}$ where y_{ij}= response variable score because of treatment i^{th} at replication j^{th}; μ = mean of population; ε_{ij} = experimental error because of treatment i^{th} at replication j^{th}. The hypotheses of the design were $H_0: \tau_1 = \tau_2 = \cdots \tau_t = 0$ and H_1: minimal one pairs $\tau_1 \neq \tau_2$. The decision null hypothesis was rejected if *F*-value was greater than *F* table or *p*-value was less than alpha. Moreover, a Duncan's test was carried out to find out the significant pairs.

Figure 2. Visual appearance of (A) extract of *Calotropis gigantea* leaves; (B) AgNPs-LCg solution before incubation; (C) AgNPs-LCg solution after incubation. The AgNPs-LCg hybridized either with PO—crude or hydrolate, light fraction and heavy fraction have very similar visual appearance as presented in panel D.

Table 2. ANOVA analysis for response surface model

Source	Degree of freedom	Adjusted sum of square	Adjusted mean square	*F*-value	*p*-value
Model	5	6853.04	1370.61	175.53	<0.001
Linear	2	607.84	303.92	38.92	<0.001
$AgNO_3$ concentration	1	183.21	183.21	23.46	0.002
pH	1	424.63	424.63	54.38	<0.001
Square	2	5020.19	2510.10	321.47	<0.000
$AgNO_3$ concentration*$AgNO_3$ concentration	1	1437.50	1437.50	184.10	<0.000
pH*pH	1	4133.15	4133.15	529.34	<0.000
2-way interaction	1	1225.00	1225.00	156.89	<0.000
$AgNO_3$ concentration*pH	1	1225.00	1225.00	156.89	<0.000
Error	7	54.66	7.81		
Lack-of-fit	3	54.66	18.22	Undefined	Undefined
Pure error	4	0.00	0.00		
Total	12	6907.69			

There is the effect of linear, square, and two-way interaction on SPR (**Table 2**). The R-square was utilized to ascertain the level of agreement of the data within the model [44]. An R-square of 98.64% indicates that this model can explain 98.64% of the SPR variation. In the response surface regression, the SPR is influenced by $AgNO_3$ concentration, pH, $AgNO_3$ concentration^2, pH^2, and the interaction between $AgNO_3$ concentration and pH at alpha 0.01. The correlation between the silver precursor concentration, pH, and the defined response variable (SPR wavelength) was further elucidated through 3D surface and contour plots, as depicted in **Figure 3A** and **Figure 3B**.

Antimicrobial activity assay

The antimicrobial activity testing is presented in **Figure 4**. Antimicrobial activity testing was performed in triplicate, resulting in the presentation of inhibition zone data as mean ± standard deviation (SD). According to the data in **Table 3**, the wastewater from the distillation process of *P. cablin*, used in the green synthesis hybrid to form PH-AgNPs-LCg, increased the antibacterial activity against *E. coli* by 0.19 mm, though it did not enhance activity against *S. aureus* and *C. albicans*. Crude PO, sourced directly from farmers, was found to augment the antimicrobial activity of AgNPs-LCg against *S. aureus, E. coli,* and *C. albicans* by 1.28 mm, 1.55 mm, and 0.24 mm, respectively. Further, the purification of PO into light and heavy fractions was observed to enhance antimicrobial activity more than the crude PO. Specifically, the light fraction of PO improved the antimicrobial efficacy of AgNPs-LCg against *S. aureus, E. coli,* and *C. albicans* by 1.8 mm, 0.95 mm, and 0.65 mm, respectively, while the heavy fraction showed increases of 2.8 mm, 1.15 mm, and 1.02 mm against the same microbes. Based on the results obtained, HP-AgNPs-LCg emerged as the hybrid green synthesis result with the highest antimicrobial activity. Therefore, HP-AgNPs-LCg will be characterized in the next stage.

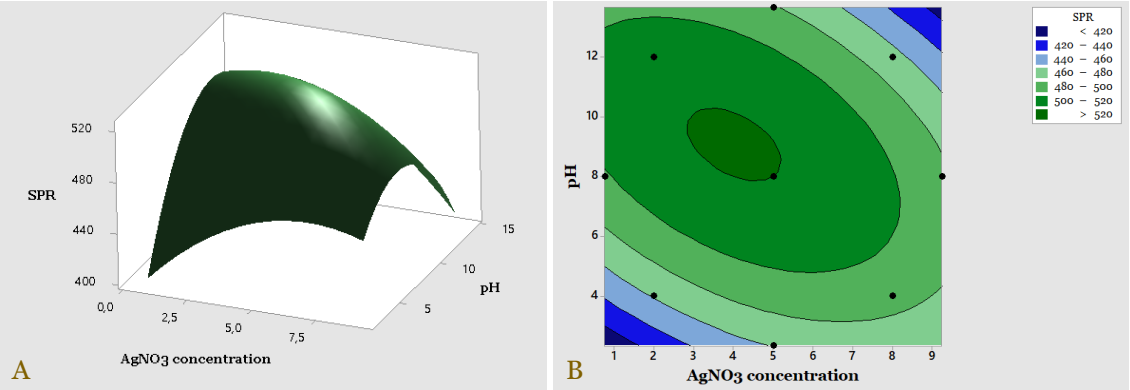

Figure 3. (A) 3-D response surface and (B) 2-D contour plot illustrating the relationship between $AgNO_3$ concentration, pH, and surface plasmon resonance (SPR) of AgNPs-LCg.

Table 3. Inhibition zones of AgNPs resulting from green synthesis and hybrid green synthesis against *S. aureus, E. coli*, and *C. albicans*

Sample	Inhibition zone, mean±SD (mm)		
	Staphylococcus aureus	*Escherichia coli*	*Candida albicans*
AgNPs-LCg	10.47±0.17^{e}	11.37±0.55^{d}	7.07±0.04^{cd}
Calotropis gigantea leaf extract	0.00±0.00^{f}	0.00±0.00^{e}	0.00±0.00^{e}
PO-AgNPs-LCg	11.75±0.58^{d}	12.92±0.82^{c}	7.31±0.43^{cd}
PH-AgNPs-LCg	10.66±0.39^{e}	11.35±0.58^{d}	6.03±0.05^{e}
HP-AgNPs-LCg	13.27±0.16^{c}	12.52±0.54^{c}	8.09±0.11^{c}
LP-AgNPs-LCg	12.27±0.13^{d}	12.32±0.30^{c}	7.72±0.29^{d}
Patchouli oil	13.96±0.62^{b}	15.27±0.14^{b}	9.44±0.40^{b}
Control	16.00±0.10^{a}	23.14±0.82^{a}	34.18±1.23^{a}

The controls used for *S. aureus, E. coli,* and *C. albicans* are vancomycin, gentamicin, and ketoconazole, respectively; The mean values with the same letter indicate no significant difference.

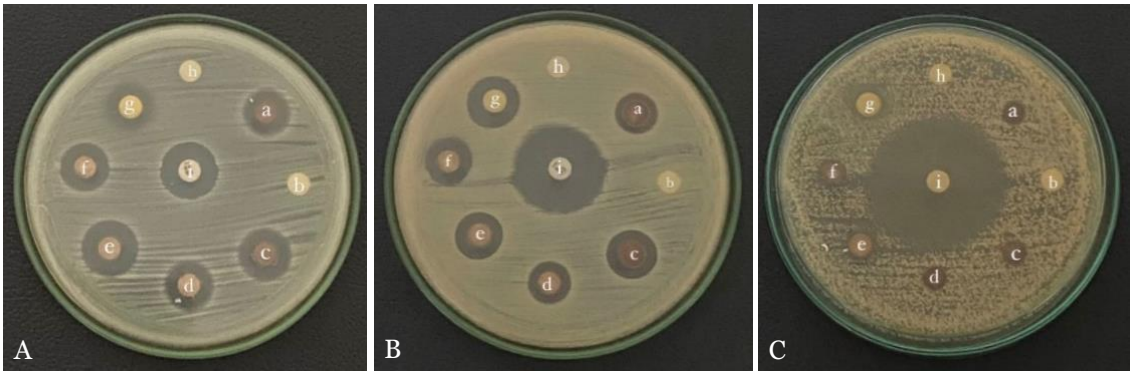

Figure 4. Antimicrobial activity analysis: (A) *Staphylococcus aureus*; (B) *Escherichia. coli* and (C) *Candida albicans* (where, a: AgNPs-LCg, b: *Calotropis gigantea* leaf extract, c: PO-AgNPs-LCg, d: PH-AgNPs-LCg, e: HP-AgNPs-LCg, f: LP-AgNPs-LCg, g: patchouli oil, h: negative control, and i: positive control).

UV-Vis and FTIR characterization

AgNPs produced using plant bioreductors typically exhibit maximum absorption within the range of 420-455 nm, attributable to the SPR phenomenon [42]. The absorbance measurements of our samples are presented in **Figure 5A**. Based on this data, the SPRs for AgNPs-LCg and HP-AgNPs-LCg were identified at 400 nm and 360 nm, respectively.

FTIR spectroscopy is widely utilized to identify surface functional groups in nanoparticles [2]. The FTIR characterization results from this study are depicted in **Figure 5B**. The spectral profiles of all samples indicated the existence of O—H stretching, C=C stretching, N—H bending, and C—H bending vibrations, corresponding to the absorbance peaks detected at 3250, 2100, 1600, and 610 cm^{-1}, respectively.

A B

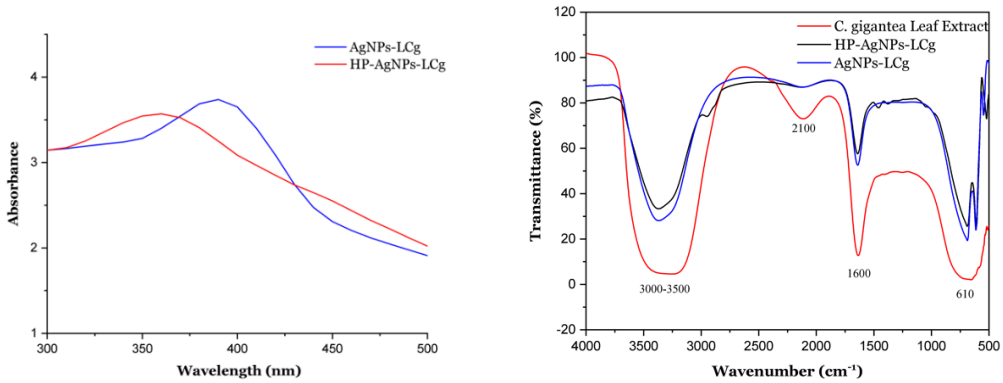

Figure 5. (A) UV–Vis spectrophotometry characterization and (B) Fourier transform infrared (FTIR) spectra of AgNPs resulting from green synthesis and hybrid green synthesis.

Particle size of AgNPs-LCg and HP-AgNPs-LCg

The particle measurements using PSA indicate that AgNPs-LCg and HP-AgNPs-LCg were found to have the smallest sizes of 56 and 422 nm, respectively (**Figure 6**). The AgNPs-LCg in this study were obtained within the size range of 1–100 nm, hence can be claimed as NPs. HP-AgNPs-LCg were obtained in larger sizes due to the additional layer of oil coating the particles.

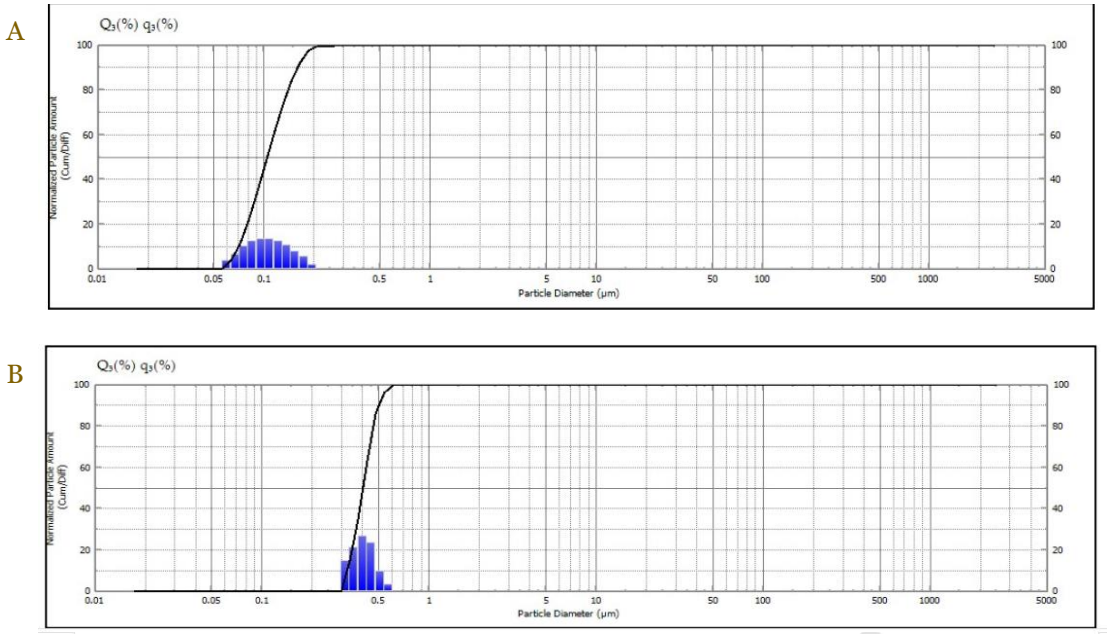

Figure 6. Particle size distribution using particle size analyzer of (A) AgNP-LCg and (B) HP-AgNP-LCg.

Morphology of AgNPs-LCg and HP-AgNPs-LCg

SEM analysis revealed that while most AgNPs-LCg were spherical and monodisperse, others were shapeless aggregates (**Figure 7a**). HP-AgNPs-LCg predominantly appeared cubic with some spherical forms (**Figure 7b**), along with some irregularly shaped particles and minimal agglomerations. The energy-dispersive X-ray spectroscopy (EDS) technique was employed to analyze the elemental composition of biosynthesized AgNPs in solution, revealing silver metal with a strong signal and a weight percent of 56.49%, indicating the presence of metallic silver nanocrystals (**Figure 9a**) and confirming the successful synthesis of AgNPs using *C. gigantea* leaf extract. The results indicate that the dominance of silver in our samples confirms they are indeed silver nanoparticles, thereby eliminating the need for further XRD testing to prove the presence of silver metal. Furthermore, HP-AgNPs-LCg displayed additional elements, calcium (2.57%) and potassium (3.74%), likely originating from the heavy fraction of PO (**Figure 8**).

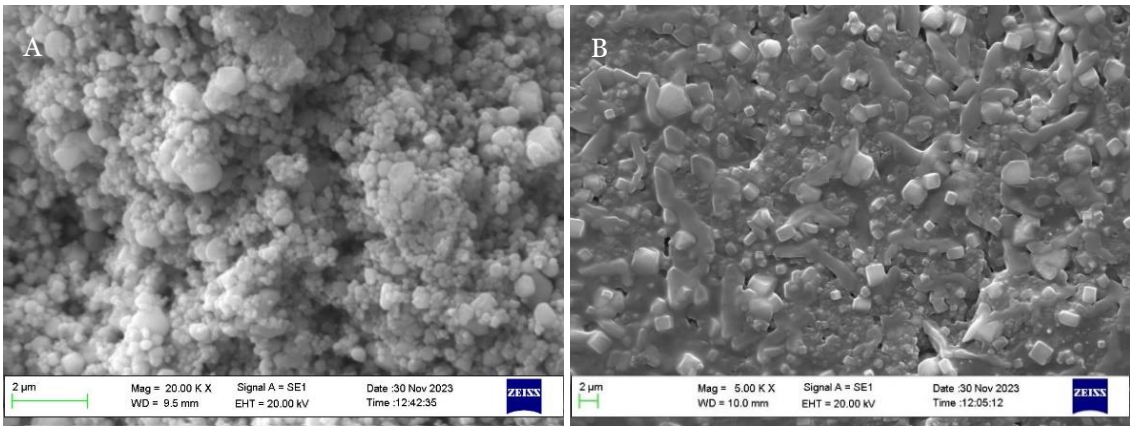

Figure 7. Scanning electron microscopy (SEM) images of AgNPs-LCg (A) and HP-AgNPs-LCg (B) were displayed at 20,000× and 50,000× magnification, respectively.

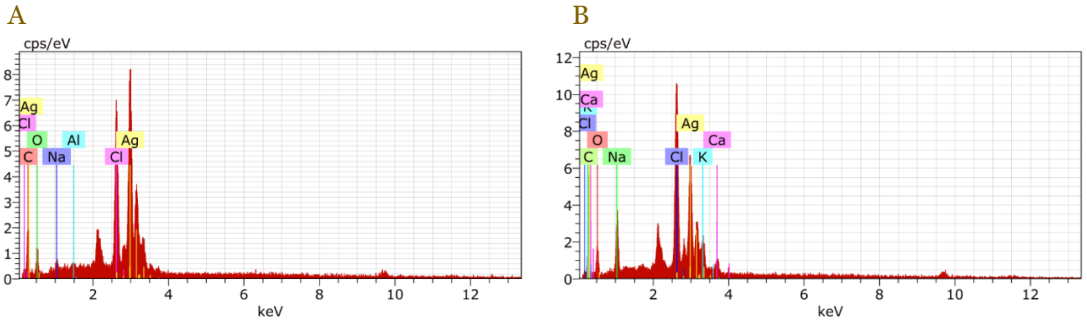

Figure 8. Energy-dispersive X-ray spectroscopy (EDS) spectra of (a) AgNPs-LCg and (b) HP-AgNPs-LCg.

Discussion

Plants thriving in extreme environments often develop robust natural defenses to cope with adverse conditions [39-42]. They produce chemical or bioactive compounds to combat environmental stress, pathogen attacks, or predation. These compounds can possess significant pharmacological properties, making them valuable for medicinal purposes. For these reasons, we selected *C. gigantea* from a geothermal area where surface temperatures of geothermal fluids reach 84°C and the pH is 6.61. The *C. gigantea*, being the most abundant and robust plant in this region, is particularly noted for its leaves' capacity to reduce silver metal [29]. We extracted the leaf samples using a common aqueous solvent method [25,26,43-47]. The green synthesis of AgNPs-LCg was conducted by reacting $AgNO_3$ with *C. gigantea* leaf extract. Several studies claim that a color change before and after the reaction to brown indicates the successful green synthesis of AgNPs. The reduction of Ag^+ to Ag^0 is indicated by a change in the solution's color to yellowish-brown [42,45] or reddish brown [30,46,47]. The addition of patchouli oil in this study did not significantly alter the color of the synthesized AgNPs solution (**Figure 2**). The AgNPs solution hybridized with patchouli oil appears oily and non-homogeneous.

Reaction optimization using RSM was conducted by observing the correlation between the silver precursor concentration and pH as independent variables and the defined response variable (SPR wavelength) (**Figure 3**). An in-depth analysis of these graphs indicated a direct correlation between the tested parameters and the observed SPR. Especially, the positioning of the SPR band significantly influences the particle size; as the particle size diminishes, the absorption maximum shifts towards shorter wavelengths [48]. Moreover, nanoparticles of smaller size tend to exhibit a more pronounced antibacterial response compared to their larger counterparts. This phenomenon is likely attributable to the increased surface area to volume ratio, enhancing the interaction between the nanoparticles and the bacterial cell wall. The reduced size also enables nanoparticles to more effectively penetrate the cellular interstitium, leading to increased bacterial mortality [49]. Consequently, analyzing the SPR band with shorter

wavelengths is crucial for synthesizing AgNPs-LCg, thereby producing smaller nanoparticles. Numerical optimization revealed that an SPR band with maximum absorption at 400 nm is attainable at an $AgNO_3$ concentration of 4 mM and a pH of 9.

Antimicrobial activity tests were performed on various samples of green synthesis hybrid AgNPs. It was noted that $AgNO_3$ exhibited the least inhibition against pathogenic microorganisms [50]. Similarly, in this study, the *C. gigantea* leaf extract from the Ie Seu-um geothermal area showed no antimicrobial activity, as illustrated in **Figure 4**. The plant extracts tested were used directly from the extraction stage without any further concentration process. Contrarily, another study reported that *C. gigantea* leaf extract exhibited antifungal activity against *C. albicans* with an MIC value of 200 µg/mL [31]. However, in our current research, AgNPs-LCg demonstrated antimicrobial activity against *S. aureus, E. coli,* and *C. albicans*, with inhibition zones measuring 10.47±0.17 mm, 11.37±0.55 mm, and 7.07±0.04 mm, respectively (**Table 3**). For comparison, in a previous study, AgNPs-LCg synthesized using 9 mM $AgNO_3$ (the maximum concentration used in that study) showed antimicrobial activity against the same organisms with inhibition zones of 10.60±0.22 mm, 8.40±0.33 mm, and 8.09±0.25 mm, respectively [36]. This comparison indicates that the optimization of the reaction using the RSM approach in our study was successful not only in achieving smaller particle sizes but also in enhancing antibacterial activity against Gram-negative bacteria and fungi.

The HP-AgNPs-LCg exhibited the highest average values for *S. aureus, E. coli,* and *C. albicans* compared to other AgNP samples. The results obtained from the Duncan's test indicate that LP-AgNPs-LCg and PO-AgNPs-LCg have average values for *S. aureus* and *E. coli* that are not significantly different.

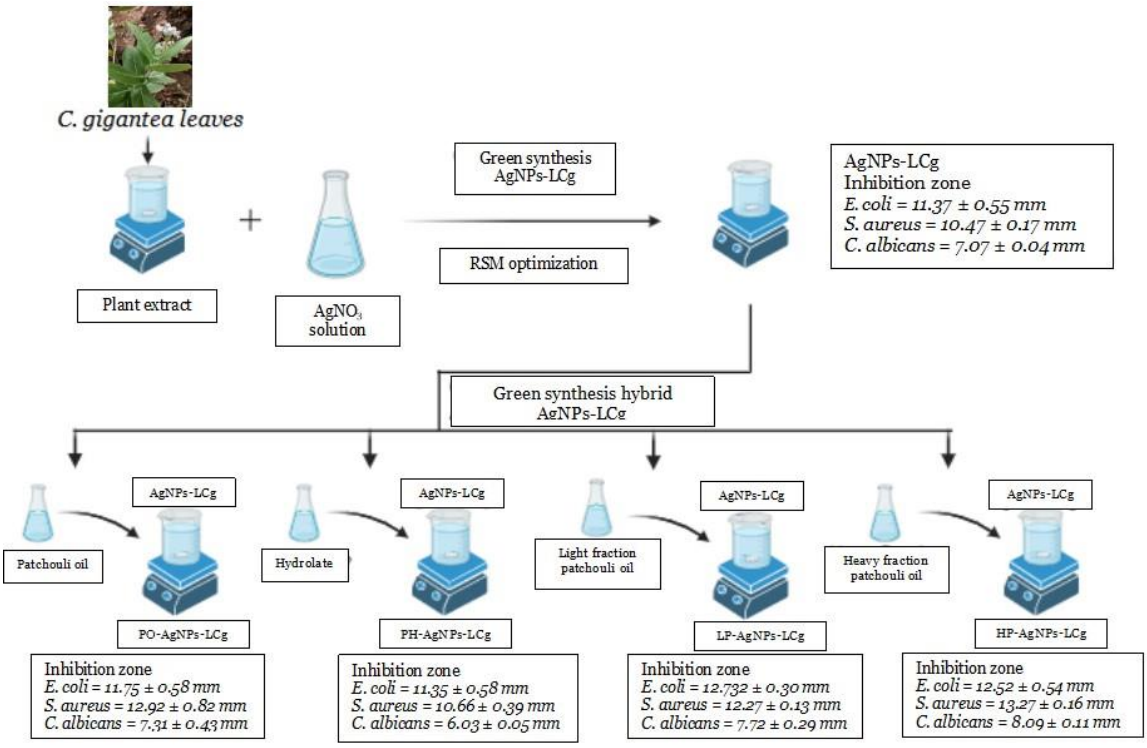

Figure 9. The results of antimicrobial testing on samples of AgNPs-LCg from green synthesis and hybrid green synthesis.

PO has been found to be more effective against Gram-positive bacteria than Gram-negative bacteria [51,52]. In this study, the PO used as a coating for AgNPs-LCg included crude PO obtained from local farmers, hydrolate, and PO fractionated into heavy and light fractions. The *P. cablin*, cultivated in Sabang City, Aceh Province, Indonesia, was distilled by farmers to produce crude PO, with hydrolate as a by-product. This crude PO was then further separated into light and heavy fractions. This study's novel finding is that PO in any form can enhance antimicrobial activity. This enhancement was not limited to Gram-negative bacteria, as previously reported [34], but also extended to Gram-positive bacteria and fungi (**Figure 9**). Among the four types of

PO used, the heavy fraction was the most effective in enhancing the antimicrobial properties of AgNPs-LCg against all tested microorganisms. That is why we only characterized HP-AgNPs-LCg in the next discussion. Further research is recommended to elucidate the mechanisms through which the light and heavy fractions of PO enhance the antimicrobial activity of AgNPs. Our findings indicated that purified PO yields higher antibacterial and antifungal activity compared to crude PO. Additionally, we hypothesize that the differing components between the light and heavy fractions of PO contribute to their varying effectiveness.

AgNPs are known to generate reactive oxygen species (ROS) such as hydroxyl and superoxide radicals, which induce oxidative stress in cells, leading to significant damage or even death of microbial cells [53]. The predominant mechanisms of antibacterial activity in metal nanoparticles, including AgNPs, are often attributed to oxidative stress linked with ROS production, metal ion release, and various non-oxidative processes. Non-oxidative mechanisms reported in the literature encompass direct interactions with the cell wall and membrane, penetration into the cell, and subsequent inhibition of nucleic acid and protein synthesis, along with modulation of gene expression [54]. Furthermore, Ag^{+} ions emanating from AgNPs are known to bind to sulfhydryl groups in proteins, leading to their denaturation [22]. AgNPs are also understood to adhere to the bacterial respiratory chain, disrupting vital physiological processes and ultimately causing cell death [22]. Another study highlights that bacterial cell membranes, containing sulfur-bearing proteins and amino acids both inside and outside, allow silver to interact with them, resulting in bacterial inactivation. In this context, silver ions released from AgNPs are known to interact with phosphorus in DNA and sulfur-containing proteins, inhibiting enzyme activity [55].

The characterization conducted for both AgNPs-LCg and HP-AgNPs-LCg samples included UV-Vis spectrophotometry, FTIR, PSA, and SEM-EDX. Based on absorbance measurements using UV-Vis spectrophotometry, the SPRs for AgNPs-LCg and HP-AgNPs-LCg were identified at 400 nm and 360 nm, respectively (**Figure 5A**). These findings are in close alignment with other reported SPR observations. AgNPs synthesized using *H. perforatum, N. sativa, Andrographis paniculata, Phyllanthus niruri, Tinospora cordifolia,* and *C. gigantea* exhibited SPRs at 401, 400, 425, 424, 452, and 422 nm, respectively [26,30,42,56]. Additionally, the SPR of AgNPs-LCg in this study was observed at a shorter wavelength compared to our previous study [36], which is indicative of the smaller particle size achieved. The size of AgNPs is correlated with the SPR peak, as lower SPR wavelengths correspond to smaller particle sizes [48].

The detection of specific constituents is crucial as biochemical and biomolecular components are known to play a primary role in the reduction of metal ions to nanoparticles [3]. We observed that O—H stretching, C=C stretching, N—H bending, and C—H bending vibrations, which are inherent functional groups in *C. gigantea* leaf extract, were also present in both AgNPs-LCg and HP-AgNPs-LCg samples (**Figure 5B**). This indicated their significant role in the reduction process of Ag. Additionally, O-H and amino acid groups have been identified as components acting as capping agents, stabilizing the AgNPs [57]. Another study also indicated that AgNP-LCg samples exhibit amide, amino acid, and alkane groups, which are evident in their respective spectral peaks at 1116, 1457, 1629, 2361, 2853, 2923, and 3421 cm^{-1} [31].

The AgNPs-LCg were obtained with a minimum size of 56 nm, which is smaller than the particle sizes observed in our previous study [36]. This reduction in size indicated the success of the optimization method using the RSM. The AgNPs-LCg samples were found to be spherical in shape, as reported in our earlier work [36]. The green synthesis hybrid AgNPs are characterized by an outer PO layer, which contributes to the formation of an additional coating on the nanoparticles [34]. This coating process, particularly the application of PO to AgNPs-LCg, is known to increase the particle size. Specifically, HP-AgNPs-LCg exhibited a predominant particle size at 422 nm. It is hypothesized in this study that the coating process contributed to the larger size of HP-AgNP-LCg compared to AgNP-LCg. The variation in size and form of the nanoparticles can be attributed to the presence of multiple phytoconstituents in the plant extract, which act as reducing agents [58].

SEM analysis revealed that while most AgNPs-LCg were spherical and monodisperse, others were shapeless aggregates (**Figure 7A**), similar to plant-synthesized AgNPs reported in previous studies using *H. perforatum* [26], *N. sativa* [56], *Platycodon grandiflorum* [45], *A. paniculata,*

P. niruri, and *T. cordifolia* [42]. HP-AgNPs-LCg predominantly appeared cubic with some spherical forms (**Figure 7B**), along with some irregularly shaped particles and minimal agglomerations, likely caused by residual oil layers. The heavy fraction of PO coating on AgNPs-LCg resulted in aggregation, similar to the aggregation seen with St. John's wort extract, which acts as a protective capping layer on silver nanoparticles [26]. The EDS characterization (**Figure 8**) showing silver as the dominant metal clearly indicates that the produced nanoparticles are confirmed to be silver nanoparticles.

The characteristics of AgNPs and their antimicrobial abilities, particularly when synthesized using *C. gigantea* leaves from the geothermal area of Ie Seu-um in Aceh Besar District, Aceh Province, Indonesia, highlight their potential as eco-friendly antimicrobial agents. The successful enhancement of antimicrobial activities through the incorporation of PO suggests a promising avenue for the development of sustainable solutions to combat microbial resistance. Leveraging local resources underscores the importance of environmentally conscious approaches in addressing global health challenges. While this study provides valuable insights into the potential antimicrobial synergy of green nanotechnology, several limitations must be acknowledged. Firstly, the focus of this research is solely on the antimicrobial activity of AgNPs resulting from green synthesis using *C. gigantea* leaves enhanced by PO. Secondly, the parameters and experimental condition variations may not account for the entire complexity of interactions between raw materials and reaction conditions. Thirdly, the antimicrobial activity tests were conducted in vitro and did not include testing on animal or clinical models.

Conclusion

This study revealed that the incorporation of PO, in its various forms, effectively augmented the antimicrobial activity of AgNPs-LCg, making them more potent against both Gram-positive and Gram-negative bacteria, as well as fungi. This enhancement can be attributed to the synergistic effects of the bioactive compounds present in PO and the inherent properties of AgNPs-LCg. The outcomes of this research open new avenues for the development of more efficient and eco-friendly antimicrobial agents, leveraging the natural resources of Aceh Province, Indonesia. Further studies are recommended to explore the underlying mechanisms of action and to optimize the formulation for potential commercial applications. The positive results of this study hold significant promise for the advancement of green synthesis approaches in the field of antimicrobial research.

Ethics approval

Not required.

Competing interests

All the authors declare that there are no conflicts of interest.

Funding

This research was funded by Universitas Syiah Kuala, Kementerian Pendidikan, Kebudayaan, Riset dan Teknologi Indonesia through "Program Riset Unggulan USK Percepatan Doktor" grant number 539/UN11.2.1/PT.01.03/PNBP/2023.

Underlying data

Derived data supporting the findings of this study are available from the corresponding author on request.

How to cite

Kemala P, Khairan K, Ramli M, *et al.* Optimizing antimicrobial synergy: Green synthesis of silver nanoparticles from *Calotropis gigantea* leaves enhanced by patchouli oil. Narra J 2024; 4 (2): e800 - http://doi.org/10.52225/narra.v4i2.800.

References

1. Szewczuk MA, Zych S, Oster N, *et al.* Activity of patchouli and tea tree essential oils against staphylococci isolated from pyoderma in dogs and their synergistic potential with gentamicin and enrofloxacin. Animals 2023;13(8):(1279).
2. Pryshchepa O, Pomastowski P, Buszewski B. Silver nanoparticles : Synthesis, investigation techniques, and properties. Adv Colloid Interface Sci 2020;284:87-100.
3. Chan SS, Low SS, Chew KW, *et al.* Prospects and environmental sustainability of phyconanotechnology: A review on algae-mediated metal nanoparticles synthesis and mechanism. Environ Res 2022;212(Pt A):113140.
4. Ningsih DS, Idroes R, Bachtiar BM, *et al.* Clinical and oral microbiome pattern of halitosis patients with periodontitis and gingivitis. Narra J 2023;3(2):e163.
5. Khairan K, Septiya S, Murniana. Antibacterial activity of magnolia alba flower extracts on staphylococcus epidermidis and staphylococcus aureus. IOP Conf Ser Earth Environ Sci 2021;711(1):012017.
6. Khairan K, Astuti Y, First IS. Gel formulation of ethyl acetate garlic extraction and its activity against staphylococcus epidermis. J Chem Nat Resour 2019;1(2):69-78.
7. Abas AH, Tallei TE, Idroes R, *et al.* Ficus minahassae (Teijsm & de Vriese) Miq.: A fig full of health benefits from North Sulawesi, Indonesia: A mini review. Malacca Pharm 2023;1(1):1-7.
8. Rahmad R, Earlia N, Nabila C, *et al.* Antibacterial cream formulation of ethanolic Pliek U extracts and ethanolic residue hexane Pliek U extracts against S*taphylococcus aureus*. IOP Conf Ser: Mater Sci Eng 2019;523:012011.
9. Rahu MI, Naqvi SHA, Memon NH, *et al.* Determination of antimicrobial and phytochemical compounds of Jatropha curcas plant. Saudi J Biol Sci 2021;28(5):2867-2876.
10. Seleteng-kose L, Moteetee A, Vuuren S Van. South African journal of botany medicinal plants used for the treatment of sexually transmitted infections in the Maseru District, Lesotho: Antimicrobial validation, phytochemical and cytotoxicity studies. South Afr J Bot 2019;122:457-466.
11. Fakri F, Harahap SP, Muhni A, *et al.* Antimicrobial properties of medicinal plants in the lower area of Ie Seu-um geothermal outflow, Indonesia. Malacca Pharm 2023;1(2):55-61.
12. Mousavi SS, Karami A, Haghighi TM, *et al.* In silico evaluation of Iranian medicinal plant phytoconstituents as inhibitors against main protease and the receptor-binding domain of sars-cov-2. Molecules 2021;26(18):5724.
13. Tallei TE, Tumilaar SG, Niode NJ, *et al.* Potential of plant bioactive compounds as SARS-CoV-2 main protease (Mpro) and spike (S) glycoprotein inhibitors: A molecular docking study. Scientifica 2020;2020:6307457.
14. Imelda E, Fitria U, Mutia UP, *et al. Hippobroma longiflora* L Leaves as a natural inhibitor of cataract progression: A comprehensive study integrating ethanol extract, HPLC, and molecular docking approaches. Grimsa J Sci Eng Technol 2023;1(2):40-51.
15. Muchtaromah B, Firdaus AMK, Ansori ANM, *et al.* Effect of pegagan (*Centella asiatica*) nanoparticle coated with chitosan on the cytokine profile of chronic diabetic mice. Narra J 2024;4(1):e697.
16. Muchtaromah B, Wahyudi D, Ahmad M, *et al.* Chitosan-tripolyphosphate nanoparticles of mango ginger (Curcuma mangga) extract: Phytochemical screening, formulation, characterization, and antioxidant activity. Pharmacogn J 2021;13(5):1065-1071.
17. Fadholly A, Ansori ANM, Proboningrat A, *et al.* Apoptosis of hela cells via caspase-3 expression induced by chitosan-based nanoparticles of Annona squamosa leaf extract: In vitro study. Indian J Pharm Educ Res 2020;54(2):416-421.
18. Khalid A, Asghar A, Danish M, *et al.* Effectivity and safety after intravitreal triamcinolone acetonide and bevacizumab titanium dioxide (TiO2) nanoparticles induced gonadal toxicity in exposed male sprague-dawley rats. J Med Chem Sci 2023;7(1):150-165.
19. Kakakhel MA, Sajjad W, Wu F, *et al.* Green synthesis of silver nanoparticles and their shortcomings, animal blood a potential source for silver nanoparticles: A review. J Hazard Mater Adv 2021;1(1):100005.
20. Yonathan K, Mann R, Mahbub KR, *et al.* The impact of silver nanoparticles on microbial communities and antibiotic resistance determinants in the environment. Environ Pollut 2022;293:118506.
21. Sharma NK, Vishwakarma J, Rai S, *et al.* Green route synthesis and characterization techniques of silver nanoparticles and their biological adeptness. ACS Omega 2022;7(31):27004-27020.
22. Abass SM, Sunitha S, Ashaq SM, *et al.* An overview of antimicrobial and anticancer potential of silver nanoparticles. J King Saud Univ - Sci 2022;34(2):101791.
23. Tanase C, Berta L, Coman A, *et al.* Antibacterial and antioxidant potential of silver nanoparticles biosynthesized using the spruce bark extract. Nanomaterials 2019;9(11):1541.

24. Alkhathlan AH, Al-abdulkarim HA, Khan M, *et al.* Ecofriendly Synthesis of silver nanoparticles using aqueous extracts of *Zingiber officinale* (Ginger) and *Nigella sativa* L. Seeds (Black cumin) and comparison of their antibacterial potential. Sustainability 2020;12:10523.
25. Govindan L, Anbazhagan S, Altemimi AB, *et al.* Efficacy of antimicrobial and larvicidal activities of green synthesized silver nanoparticle using leaf extract of *Plumbago auriculata* Lam. Plants 2020;9(11):1577.
26. Alahmad A, Al-zereini WA, Hijazin TJ, *et al.* Green synthesis of silver nanoparticles using *Hypericum perforatum* L. Aqueous extract with the evaluation of its antibacterial activity against clinical and food pathogens. Pharmaceutics 2022;14(5):1104.
27. Mahmud KM, Hossain MM, Polash SA, *et al.* Investigation of antimicrobial activity and biocompatibility of biogenic silver nanoparticles synthesized using syzigyum cymosum extract. ACS Omega 2022;7(31):27216-27229.
28. Shumi G, Demissie TB, Eswaramoorthy R, *et al.* Biosynthesis of silver nanoparticles functionalized with histidine and phenylalanine amino acids for potential antioxidant and antibacterial activities. ACS Omega 2023;8(27):24371-24386.
29. Kabir SR, Asaduzzaman AKM, Amin R, *et al.* Zizyphus mauritiana fruit extract-mediated synthesized silver/silver chloride nanoparticles retain antimicrobial activity and induce apoptosis in MCF-7 cells through the fas pathway. ACS Omega 2020;5(32):20599-20608.
30. Mathew S, Victo CP, Sidhi J, *et al.* Biosynthesis of silver nanoparticle using flowers of *Calotropis gigantea* (L.) W.T. Aiton and activity against pathogenic bacteria. Arab J Chem 2020:13:9139-9144.
31. Ali EM, Abdallah BM. Effective inhibition of candidiasis using an eco- friendly leaf extract of calotropis-gigantean-mediated silver nanoparticles. Nanomaterials 2020;10(422):1-16.
32. Sorubavalli U, Vadivazhagi MK, Vadivelu J. Antioxidant and antimicrobial activity of calotrophis mediated silver nanoparticles. J Compos Theory 2019;XII(X):303-312.
33. Kemala P, Khairan K, Ramli M, *et al.* Characterizing the size distribution of silver nanoparticles biofabricated using calotropis gigantea from geothermal zone. Heca J Appl Sci 2023;1(2):30-36.
34. Parmar A, Kapil S, Sachar S, *et al.* Design of experiment based methodical optimization and green syntheses of hybrid patchouli oil coated silver nanoparticles for enhanced antibacterial activity. Curr Res Green Sustain Chem 2020;3(June):100016.
35. Arahman N, Rosnelly CM, Windana DS, *et al.* Antimicrobial hydrophilic membrane formed by incorporation of polymeric surfactant and patchouli oil. Polymers 2021;13(22):3872.
36. Kemala P, Idroes R, Khairan K, *et al.* Green synthesis and antimicrobial activities of silver nanoparticles using calotropis gigantea from le Seu-um geothermal area, Aceh Province, Indonesia. Mol Basel Switz 2022;27(16):1-13.
37. Kemala P, Idroes R, Khairan K, *et al.* Green Synthesis of silver nanoparticles using *Calotropis gigantea* and its characterization using UV-Vis spectroscopy. IOP Conf Ser: Earth Environ Sci 2022;951:012090.
38. Ningsih DS, Celik I, Abas AH, *et al.* Review of the ethno-dentistry activities of *Calotropis gigantea*. Malacca Pharm 2023;1(1):8-15.
39. Ajith P, Murali AS, Sreehari H, *et al.* Green synthesis of silver nanoparticles using *Calotropis gigantea* extract and its applications in antimicrobial and larvicidal activity. Mater Today Proc 2019;18:4987-4991.
40. Khairan K, Hasan M, Idroes R, *et al.* Fabrication and evaluation of polyvinyl alcohol/corn starch/patchouli oil hydrogel films loaded with silver nanoparticles biosynthesized in *Pogostemon cablin* Benth Leaves' extract. Molecules 2023;28(5):2020.
41. Gomathi M, Prakasam A, Rajkumar P V, *et al.* Green synthesis of silver nanoparticles using Gymnema sylvestre leaf extract and evaluation of its antibacterial activity. South Afr J Chem Eng 2020;32(4):1-4.
42. Sharma V, Kaushik S, Pandit P, *et al.* Green synthesis of silver nanoparticles from medicinal plants and evaluation of their antiviral potential against chikungunya virus. Appl Microbiol Biotechnol 2019;103:881-891.
43. Majeed SA, Sekhosana KE, Tuhl A. Progress on phthalocyanine-conjugated Ag and Au nanoparticles: Synthesis, characterization, and photo-physicochemical properties. Arab J Chem 2020;13(12):8848-8887.
44. Nisah K, Fahrina A, Rizki DR, *et al.* Optimization of Starch—κ-Carrageenan hybrid film as drug delivery system using response surface method. Heca J Appl Sci 2023;1(1):19-23.
45. Anbu P, Gopinath SCB, Shik H, *et al.* Temperature-dependent green biosynthesis and characterization of silver nanoparticles using balloon flower plants and their antibacterial potential. J Mol Struct 2019;1177:302-309.
46. Al-otibi F, Alkhudhair SK, Alharbi RI, *et al.* The antimicrobial activities of silver nanoparticles from and fungi. Molecules 2021;26(19):6081.
47. Haggag EG, Elshamy AM, Rabeh MA, *et al.* Antiviral potential of green synthesized silver nanoparticles of lampranthus coccineus and Malephora lutea. Int J Nanomedicine 2019;14:6217-6229.

48. Venkatachalam S. Chapter 6. Ultraviolet and visible spectroscopy studies of nanofillers and their polymer nanocomposites. Amsterdam: Elsevier; 2016.
49. Parmar A, Kaur G, Kapil S, *et al.* Biogenic PLGA-Zinc oxide nanocomposite as versatile tool for enhanced photocatalytic and antibacterial activity. Appl Nanosci Switz 2019;9(8):2001-2016.
50. Chouhan S, Guleria S. Green synthesis of AgNPs using cannabis sativa leaf extract: Characterization, antibacterial, anti-yeast and alpha-amylase inhibitory activity. Mater Sci Energy Technol 2020;3:536-544.
51. Wan F, Peng F, Xiong L, *et al. In vitro* and *in vivo* antibacterial activity of patchouli alcohol from pogostemon cablin. Chin J Integr Med 2021;27(2):125-130.
52. Kačániová M, Terentjeva M, Štefániková J, *et al.* Chemical composition and antimicrobial activity of selected essential oils against *Staphylococcus spp*. Isolated from human semen. Antibiotics 2020;9(11):765.
53. Rautela A, Rani J, Debnath (Das) M. Green synthesis of silver nanoparticles from Tectona grandis seeds extract: Characterization and mechanism of antimicrobial action on different microorganisms. J Anal Sci Technol 2019;10(1):5.
54. Maťátková O, Michailidu J, Miškovská A, *et al.* Antimicrobial properties and applications of metal nanoparticles biosynthesized by green methods. Biotechnol Adv 2022;58:107905.
55. Deshmukh SP, Patil SM, Mullani SB, *et al.* Silver nanoparticles as an effective disinfectant: A review. Mater Sci Eng C 2019;97954-965.
56. Almatroudi A, Khadri H, Azam M, *et al.* Antibacterial, antibiofilm and anticancer activity of biologically synthesized silver nanoparticles using seed extract of *Nigella sativa*. Processes 2020;8:388.
57. Mirda E, Idroes R, Khairan K, *et al.* Synthesis of chitosan-silver nanoparticle composite spheres and their antimicrobial activities. Polymers 2021;13(3990):1-13.
58. Vorobyova V, Vasyliev G, Uschapovskiy D, *et al.* Green synthesis, characterization of silver nanoparticals for biomedical application and environmental remediation. J Microbiol Methods 2022;193:106384.